Spectral effectiveness of engineered thermal cloaks in the frequency regime

David Petiteau, Sebastien Guenneau, Michel Bellieud, Myriam Zerrad, Claude Amra

Spectral effectiveness of engineered thermal cloaks in the frequency regime

David Petiteau[1], Sebastien Guenneau[1], Michel Bellieud[2], Myriam Zerrad[1] & Claude Amra[1]

[1]Aix Marseille Université, CNRS, Centrale Marseille, Institut Fresnel, UMR 7249, 13013 Marseille, France, [2]LMGC, UMR-CNRS 5508, Université Montpellier II, 34095 Montpellier Cedex 5, France.

We analyse basic thermal cloaks designed via different geometric transforms applied to thermal cloaking. We evaluate quantitatively the effectiveness of these heterogeneous anisotropic thermal cloaks through the calculation of the standard deviation of the isotherms. The study addresses the frequency regime and we point out the cloak's spectral effectiveness. We find that all these cloaks have comparable effectiveness irrespective of whether or not they have singular conductivity at their inner boundary. However, approximate cloaking with multi-layered cloak critically depends upon the homogenization algorithm and it is shown that the standard deviation varies linearly with the inverse of the number of layers.

I n 2006, Pendry, Schurig and Smith[1] showed that upon a transformation applied to a certain region of space, one could obtain a phenomenon of optical invisibility via highly heterogeneous and anisotropic meta-materials whose permittivity and permeability directly result from the space transformation. Leonhardt proposed a similar route to cloaking based upon a conformal map preserving right angles, which makes the required meta-materials isotropic[2], but this only works for a certain frequency range. Following these works, similar techniques have been used to generalize these concepts to acoustics and mechanics. In 2012, some of us proposed to extend concepts of cloaking to diffusion processes, such as heat fluxes[3], which led to first experimental demonstrations[4–7] in the transient regime. Interestingly, cloaking can be also applied to mass diffusion in a very similar manner[8] (this may open a new range of biomedical and chemical engineering[9] applications as well as light diffusion[10]).

This paper is focused on the analysis of the cloaking effectiveness in the case of heat diffusion. Indeed numerous studies point out the solution of ideal cloaking but fewer evaluate in a quantitative way the resulting effectiveness after the homogenization procedure. To reach this goal the effectiveness is here characterized by a root-mean square calculated on the line fluxes, a value which would be zero in the case of a homogeneous medium. Such characteristics allow us to compare different homogenized cloaks and emphasize their advantages and weaknesses. Moreover, rather than analyzing the effectiveness at each time step, we prefer to perform a spectral analysis, on the basis of the classical time-frequency analogy. Hence we work in the frequency or time harmonic regime and investigate the spectral effectiveness of various homogenized cloaks. Such harmonic study can be implemented if one consider a heat source generated by a modulated laser beam for instance. We first investigate both ideal (singular and non singular) cloaks and approximate cloaks. Then, we improve earlier attempts to design multi-layered thermal cloaks[3,11] using the two-scale convergence method introduced in ref. 12 and further developed by ref. 13. We show that our improved design reduces by at least one order of magnitude the standard deviation of thermal isovalues compared to earlier designs. Potential applications are in thermal metamaterials and the management of heat flux.

Results

Quantitative analysis of different ideal heat cloak effectiveness Space transformation and singularities.
Changes from polar coordinates (r, θ) to radially stretched polar coordinates $(r', \theta') = (f(r), \theta)$ applied to the heat equation (19) gives us the transformed conductivity and transformed product of heat capacity and density[3]

$$\underline{\kappa}' = \kappa \mathbf{R}(\theta) \begin{pmatrix} \kappa'_{rr} & 0 \\ 0 & \kappa'_{\theta\theta} \end{pmatrix} \mathbf{R}(\theta)^T, \quad \rho'c'(r') = \rho c \frac{g(r')\frac{dg}{dr'}(r')}{r'} \quad (1)$$

where we have

$$\kappa'_{rr}(r') = \frac{g(r')}{r' \frac{dg}{dr'}(r')}, \; \kappa'_{\theta\theta}(r') = \frac{1}{\kappa'_{rr}} \qquad (2)$$

and g is the reciprocal function of the monotonic function f, $\frac{dg}{dr'}$ is the derivative function of g, $\mathbf{R}$ is the rotation matrix through an angle θ and $\mathbf{R}^T$ its transpose. Note that these parameters hold for the transformed heat equation written in time or frequency domains (see Sec. Methods). Also, in the static limit, the product $\rho'c'$ does not appear in (1), and one need only consider the anisotropic heterogeneous conductivity in (1) to obtain the desired management of heat flux. Notice that a particularly appealing application of the transformed heat equation is thermal cloaking[14]. It can be more convenient to write relations (1–2) versus the variable $r = g(r')$, with $\frac{dg}{dr'} = \frac{1}{\frac{df}{dr}}$. The result is:

$$\kappa'_{rr} = \frac{r}{f(r)} \frac{df}{dr}(r), \; k'_{\theta\theta} = \frac{1}{\kappa'_{rr}}, \; \rho'c' = \rho c \frac{r}{f(r) \frac{df}{dr}(r)} \qquad (3)$$

These last equations directly recall that singularities occur at $r' = f(r)_{|r=0}$, a radius where κ'_{rr} is zero and $\kappa'_{\theta\theta}$ infinite, while $\rho'c'$ depends on the behaviour of f around the origin. This is true whatever the transformation f though $r = 0$ does not necessarily concern the transformed region. Note in passing that a spherical (3D) diffusion cloak would have a different kind of singularity, with the radial component of the conductivity vanishing at the inner boundary of the cloak, while the other two are constant[8].

Specific transformations. Now different f functions can be used to obtain a simple design of ideal cloak by mapping a ring $\varepsilon R_1 \leq r \leq R_2$ (with $\varepsilon < \frac{R_2}{R_1}$) into another ring $R_1 \leq r' \leq R_2$. The following conditions must be fulfilled

$$f(\varepsilon R_1) = R_1, f(R_2) = R_2 \qquad (4)$$

Depending on whether $\varepsilon < 1$ or $\varepsilon > 1$, the f transformation characterizes a contraction or dilatation, respectively. A basic transformation may consist in a polynomial function $f(r) = \sum_{n=0}^{N} a_n r^n$.

Pendry's and Milton's cloaks[1,15] were based on linear ($N = 1$) and quadratic ($N = 2$) maps, respectively. Both also used $\varepsilon = 0$, which means that the whole disk $0 \leq r \leq R_2$ is transformed into the ring $R_1 \leq r' \leq R_2$. With $N = 1$ (Pendry), we obtain

$$f(r) = R_1 + r \frac{R_2 - R_1}{R_2} \qquad (5)$$

which leads to

$$\kappa'_{rr} = \frac{R_2 - R_1}{R_2} \frac{r}{R_1 + r \frac{R_2 - R_1}{R_2}} = \frac{r' - R_1}{r'} \qquad (6a)$$

$$\kappa'_{\theta\theta} = \frac{R_2}{R_2 - R_1} \frac{R_1 + r \frac{R_2 - R_1}{R_2}}{r} = \frac{r'}{r' - R_1} \qquad (6b)$$

$$\rho'c' = \rho c \frac{r}{\frac{R_2 - R_1}{R_2} \left(R_1 + r \frac{R_2 - R_1}{R_2} \right)} = \left(\frac{R_2}{R_2 - R_1} \right)^2 \frac{r' - R_1}{r'} \qquad (6c)$$

with κ'_{rr} varying in the range $\left[0, \frac{R_2 - R_1}{R_2} \right]$, $\kappa'_{\theta\theta}$ in the range

$\left[\frac{R_2}{R_2 - R_1}, +\infty \right[$ and $\rho'c'$ in the range $\left[0, \frac{R_2}{R_2 - R_1} \right]$ when $r' \in [R_1, R_2]$. We note the discontinuity of κ'_{rr}, $\kappa'_{\theta\theta}$ and $\rho'c'$ with the parameters of the surrounding medium at the interface $r' = R_2$.

With $N = 2$, one of the a_n coefficients (namely a_1 or a_2) can be arbitrarily chosen. To remove such an indetermination Milton proposed to ensure the continuity of the transformed conductivity $\underline{\underline{\kappa}}' = diag(\kappa'_{rr}, \kappa'_{\theta\theta})$ and $\rho'c'$ product at $r' = R_2$. We can see from (3) that this continuity at $r' = R_2$ amounts to ensure that $\frac{df}{dr}_{|r=R_2} = 1$ giving the following expressions on the a_n coefficients

$$a_2 = \frac{R_1}{R_2^2}, \; a_1 = 1 - 2\frac{R_1}{R_2} \text{ and } a_0 = R_1 \qquad (7)$$

This gives us

$$\kappa'_{rr} = \frac{r(2a_2 r + a_1)}{a_2 r^2 + a_1 r + a_0} \qquad (8a)$$
$$= \frac{a_1^2 + 4a_2(r' - a_0) - a_1 \sqrt{a_1^2 + 4a_2(r' - a_0)}}{2r'a_2}$$

$$\rho'c' = \rho c \frac{r}{(2a_2 r + a_1)(a_2 r^2 + a_1 r + a_0)} \qquad (8b)$$
$$= \rho c \frac{\sqrt{a_1^2 + 4a_2(r' - a_0)} - a_1}{2r'a_2 \sqrt{a_1^2 + 4a_2(r' - a_0)}}$$

and $\kappa'_{\theta\theta} = \frac{1}{\kappa'_{rr}}$. κ'_{rr} and $\kappa'_{\theta\theta}$ both vary in the range [0, 1] and we have $\rho'c' \in [0, \rho c]$ when $r' \in [R_1, R_2]$. Then, we clearly see that the continuity of κ'_{rr}, $\kappa'_{\theta\theta}$ and $\rho'c'$ is ensured at the interface $r' = R_2$ with the surrounding media.

The case $\varepsilon \neq 0$ avoids the singularity at $r' = R_1$. With $N = 1$, Kohn[16] obtained $a_1 = \frac{R_2 - R_1}{R_2 - \varepsilon R_1} > 0$ and $a_0 = (1 - \varepsilon)\frac{R_1 R_2}{R_2 - \varepsilon R_1} \neq 0$ leading to

$$\kappa'_{rr} = \frac{a_1 r}{a_1 r + a_0} = \frac{r' - a_0}{r'} \qquad (9a)$$

$$\kappa'_{\theta\theta} = \frac{a_1 r + a_0}{a_1 r} = \frac{r'}{r' - a_0} \qquad (9b)$$

$$\rho'c' = \rho c \frac{r}{a_1(a_1 r + a_0)} = \frac{r' - a_0}{a_1^2 r'} \qquad (9c)$$

with κ'_{rr} varying in the range $\left[\varepsilon \frac{R_2 - R_1}{R_2 - \varepsilon R_1}, \frac{R_2 - R_1}{R_2 - \varepsilon R_1} \right]$, $\kappa'_{\theta\theta}$ in $\left[\frac{R_2 - \varepsilon R_1}{R_2 - R_1}, \frac{R_2 - \varepsilon R_1}{\varepsilon(R_2 - R_1)} \right]$ and $\rho'c'$ in $\left[\rho c \varepsilon \frac{R_2^2}{(R_2 - \varepsilon R_1)(R_2 - R_1)}, \rho c \frac{R_2 - \varepsilon R_1}{R_2 - R_1} \right]$ when $r' \in [R_1, R_2]$. If $\varepsilon \to 0$, we retrieve the expressions from (6).

A summary of the thermal parameters' behaviour is given on Fig. 1 for different cloaks. Notice that with a general polynomial transformation the coefficients would be written as $a_n = a_n(\varepsilon, N)$. Other transformations could be used. With an exponential function we obtain $f(r) = R_1 \exp(-\mu \varepsilon R_1) \left(\frac{R_2}{R_1} \right)^{\frac{r}{R_2}}$.

Implementation and effectiveness of ideal cloaks. We study the three cloaks introduced above using the commercial finite element package COMSOL Multiphysics ®. Our two-dimensional simulation consists of the resolution of the time-harmonic heat equation (see
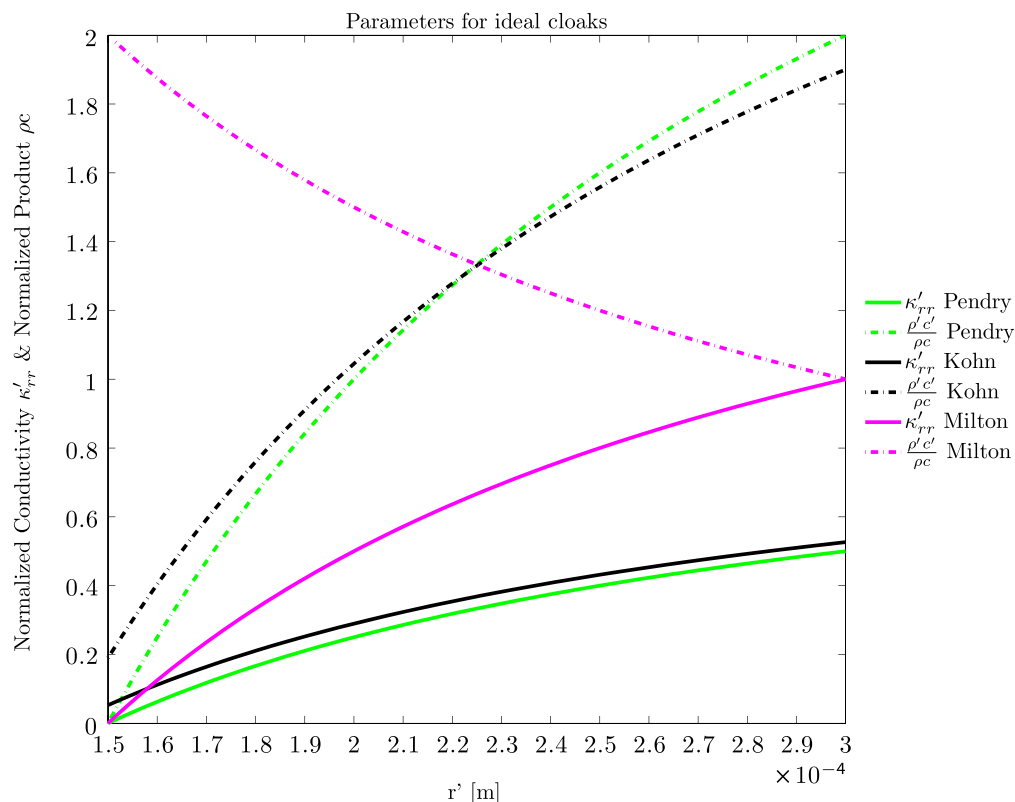
Figure 1 | Normalized conductivity κ'_{rr} and product ρc parameters used for Pendry (green), Kohn (black) and Milton (magenta) cloaks as a function of r' inside the cloak. The inner boundary of the cloak is $R_1 = 0.15$ mm and the outer boundary is $R_2 = 2R_1 = 0.3$ mm. We used here $\varepsilon = 0.1$ for Kohn's cloaks.

Sec. Methods) in a 5 mm by 0.8 mm computational domain containing the studied cloak. The medium surrounding the cloak corresponding to the region $r' \geq R_2$ is made of Titanium of thermal conductivity $\kappa_{Ti} = 22$ W.m^{-1}.K^{-1} and product of density by heat capacity $\rho c_{Ti} = 2.35 \times 10^6$ J.kg^{-1}.K^{-1} giving a thermal diffusivity $a_{Ti} \approx 1.10^{-5}$ m^2.s^{-1}. Then, the initial ring of thickness $R_2 - \varepsilon R_1$ is mapped onto the ring of thickness $R_2 - R_1$. This latter ring corresponds to the invisibility cloak whose parameters are shown on Fig. 1 depending on which transformation we choose (Pendry, Milton or Kohn). The effect of the cloak within $[R_1, R_2]$ is to straighten the isotherms for for $r' > R_2$ as if we were in an homogeneous medium. The inner and outer radii of the cloak are chosen to be respectively $R_1 = 0.15$ mm and $R_2 = 0.3$ mm. Finally, the region $0 \leq r' \leq R_1$ (mapped from the initial region $0 \leq r \leq \varepsilon R_1$) contains the cloaked object. It is made of polyvinyl chloride (PVC) of thermal conductivity $\kappa_{PVC} = 0.15$ W.m^{-1}.K^{-1} and product of density by heat capacity $\rho c_{PVC} = 1.33 \times 10^6$ J.kg^{-1}.K^{-1} of thermal diffusivity $a_{PVC} \approx 1.10^{-7}$ m^2.s^{-1}.

Notice that the 5 mm length of our computational domain has been chosen in such a way that it is in accordance with the thermal diffusion length D in Titanium at angular frequency $\omega = 1$ rad.s^{-1}, $D = \sqrt{\dfrac{2a_{Ti}}{\omega}} = 4.4$ mm. Regarding the boundary conditions, we chose to set the temperature to $T_0 = 1$ K on the left boundary of the computational domain and $T_f = 0$ K on the right boundary of the computational domain so that heat diffuses from left to right (namely from $x = -2.5$ mm to $x = 2.5$ mm). As for the upper and lower boundaries of the computational domain, we chose Neumann (perfect insulating) conditions $\dfrac{\partial T}{\partial n} = 0$.

Now the main idea to determine quantitatively the effectiveness of a cloak is to evaluate the standard deviation of the isotherms in the

vicinity of the cloak. A theoretical perfect cloak would give a zero standard deviation for all the isotherms outside the cloak as if the medium was completely homogeneous, which is clearly not the case in Fig. 2.

Thus, by evaluating the standard deviation of the isotherms (see Sec. Methods) for different cloaks, we can quantitatively determine the effectiveness of a cloak. All isotherms are calculated before and after the outer radius of the cloak in the incident diffusion direction and we define the standard deviation ratio

$$standard\ deviation\ ratio = \frac{std(bare\ object)}{std(studied\ cloak)} \qquad (10)$$

where $std(bare\ object)$ denotes the standard deviation of the isotherms when heat diffuses through the bare object to be cloaked and $std(studied\ cloak)$ is the standard deviation of the isotherms when the ideal cloak under study is around the object. An efficient cloak means that $std(studied\ cloak)$ is close to 0. Therefore the standard deviation ratio increases with increasing effectiveness.

In Fig. 3, we compare the standard deviation ratio of the isotherms resulting from a single insulating homogeneous layer made of clay of thermal conductivity $\kappa_{clay} = 1.28$ W.m^{-1}.K^{-1}, product of density by heat capacity $\rho c_{clay} = 1.28 \times 10^6$ J.kg^{-1}.K^{-1} (thermal diffusivity $a_{clay} \approx 1.10^{-6}$ m^2.s^{-1}) in red, a perfect cloak (Pendry) calculated with $\varepsilon = 0$ and $N = 1$ (green), a perfect cloak (Kohn) calculated with $\varepsilon \neq 0$ and $N = 1$ (black), and a perfect cloak based on the Milton transformation (magenta) calculated with $\varepsilon = 0$ and $N = 2$. Moreover calculation is performed at different frequencies, in a range appropriate with the thermal diffusion length and the deviation is plotted versus the average diffusion direction.

In Fig. 3, the horizontal blue line at altitude 1 is for the bare object, which is a hallmark of neutral effectiveness. We first notice that the clay monolayer cloak is below this curve, which means that the
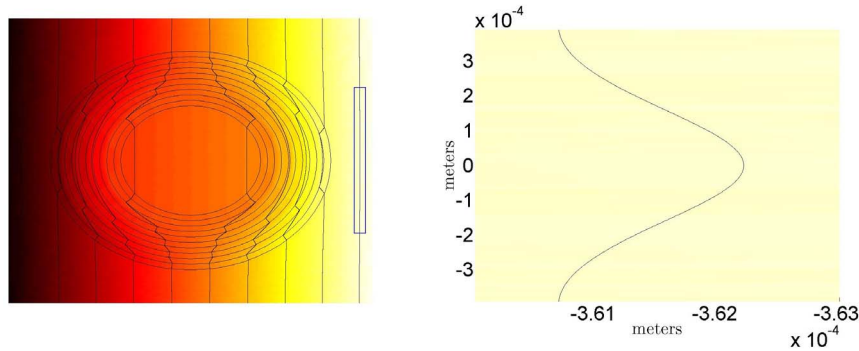
Figure 2 | Map of a thermal cloak in the static limit (left) with a close-up on the isotherms in its vicinity (right). The cloak's inner boundary is $R_1 = 0.15$ mm, and its outer boundary is $R_2 = 0.3$ mm and it consists of 10 layers of identical thickness with thermal parameters given in Table 1.

deviation has been increased. On the other hand, as expected we observe in the vicinity of the cloak that the ideal Pendry and Kohn cloaks reduce the deviation by a factor of nearly 10^5 for $\omega = 0$; rad.s^{-1}, which emphasizes a great effectiveness. The Milton cloak appears to be less efficient, but this is due to the fact that Milton's transformation is defined for a whole range of radii $R_2 \geq 2R_1$ while we considered $R_2 = 2R_1$ in our case. The Milton cloak is therefore used in a critical regime explaining its lower performances at this given mesh. A design of Milton's cloak with $R_2 > 2R_1$ reaches identical effectiveness to that of Pendry's and Kohn's cloaks as we can see in Fig. 4.

For non-zero angular frequency, the curves of effectiveness are shifted towards the zero temperature as increasing frequencies corresponds to earlier time-step in the transient regime. Thus, at greater frequencies, the temperature did not diffuse all along the computing domain and the isotherms around the cloak are close to zero. We observe a decrease of the effectiveness for all cloaks for $\omega = 0.1$, 1 and 3 rad.s^{-1} going down from 10^5 to 10^3 for the Pendry cloak for instance. This is expected as the mesh used for for the simulations were not optimized for every angular frequency, only for the static regime. Notice that optimal mesh for every angular frequency would
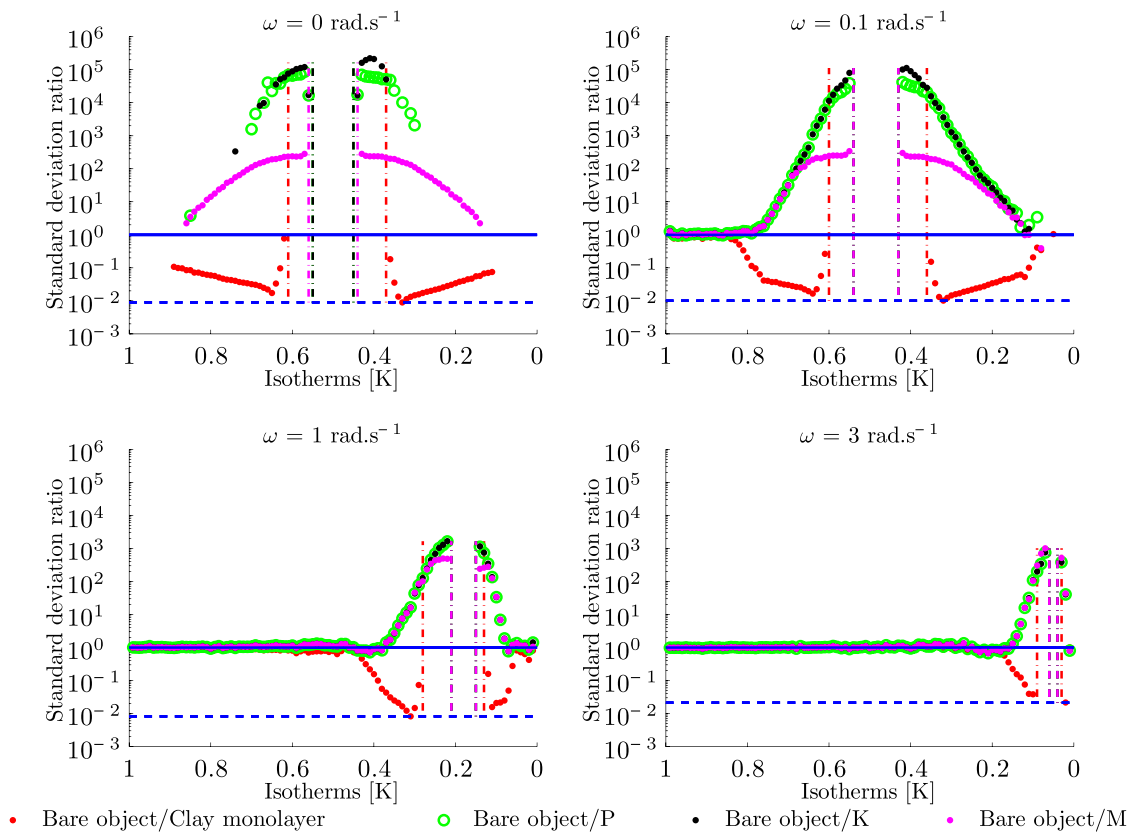

Figure 3 | Standard deviation ratio of a clay homogeneous monolayer cloak (red), Pendry's cloak (green), Kohn's cloak (black) and Milton's cloak (magenta) at angular frequencies $\omega = 0, 0.1, 1$ and 3 rad.s^{-1}. The source is on the left so that heat diffuses from left to right. The vertical lines are related to the position of the insulating layer and cloaks. The (z) vertical axis gives the ratio of the deviation on a logarithmic scale, while the (x) horizontal axis is for the temperature of the isotherms. Note that this temperature scale is directly connected to the x length coordinate. For the static regime for instance the temperature is $T = \dfrac{T_0 + T_f}{2} = 0.5$ K at half of the total x length. This is no longer the case at increasing frequencies, which explains the shift of the curves with frequency ω. The horizontal dashed blue line indicates the height of minimum of the standard deviation ratio among all the studied cloaks at frequency ω.
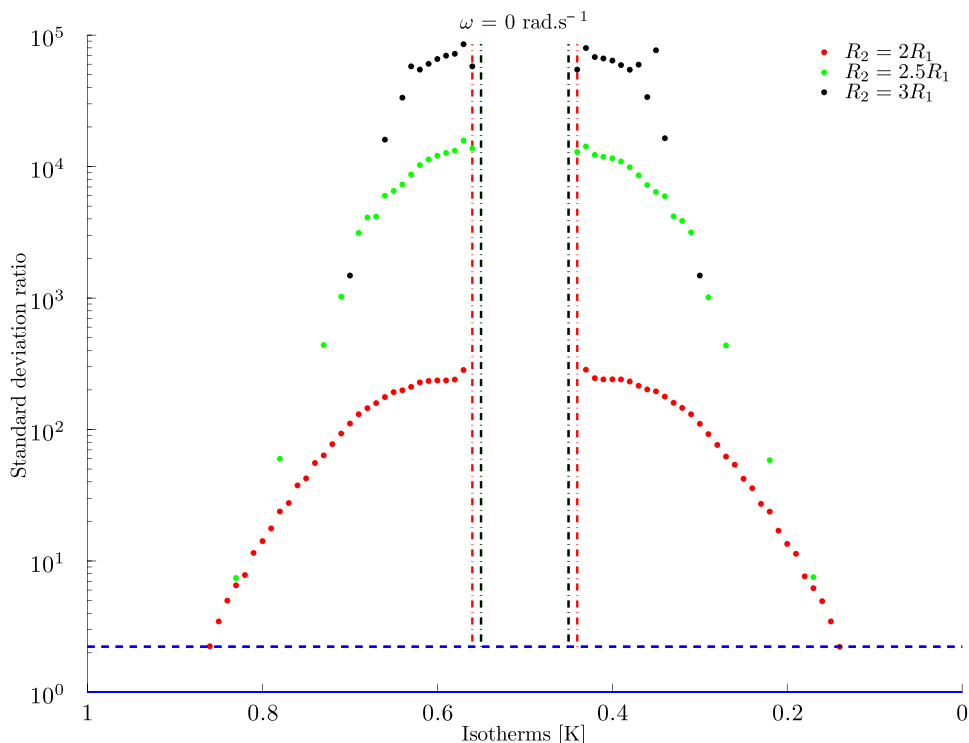
Figure 4 | Standard deviation ratio of Milton's cloaks at angular frequencies $\omega = 0$ rad.s^{-1} with $R_2 = 2R_1$ (red), $R_2 = 2.5R_1$ (green) and $R_2 = 3R_1$ (black). Note that the black curve is similar to green (Pendry's cloak) and black (Kohn's cloak) curves in the upper left panel of Fig. 3. The horizontal dashed blue line indicates the height of minimum of the standard deviation ratio among the studied Milton's cloaks.

give infinite effectiveness for all isotherms in the whole spectral range. Hence the finite effectiveness value is the result of the reference mesh we used to ensure proper finite elements calculation, and its effectiveness variation (from 10^5 to 10^3) is due to the fact that the mesh is only optimized for the static regime. Notice however that such constant mesh still allows the comparison of the different cloaks at a given mesh.

Towards homogenized multi-layered heat cloaks. We now want to build thermal cloaks that have similar properties and effectiveness as those of perfect cloaks. Thus we need a tool to design thermal metamaterials that will give the desired properties. For this purpose, we make use of the homogenization process (see Sec. Methods). We start from an alternation of concentric homogeneous thin layers with respective conductivities and product of density by heat capacity (κ_1, $\rho_1 c_1$) and (κ_2, $\rho_2 c_2$) which might depend on r'. If the number of concentric layers gets large enough (and their thicknesses vanish), this alternation will behave as the required anisotropic inhomogeneous conductivity κ' and inhomogeneous product $\rho' c'$ under certain conditions on $\kappa_1(r')$, $\kappa_2(r')$, $\rho_1 c_1(r')$ and $\rho_2 c_2(r')$:

$$\begin{cases} \dfrac{2\kappa_1(r')\kappa_2(r')}{\kappa_1(r')+\kappa_2(r')} = \kappa'_{rr} = \dfrac{g(r')}{r'g'(r')} \\ \dfrac{1}{2}\left(\kappa_1(r')+\kappa_2(r')\right) = \kappa'_{\theta\theta} = \dfrac{r'g'(r')}{g(r')} \\ \dfrac{1}{2}\left(\rho_1 c_1(r')+\rho_2 c_2(r')\right) = \rho' c' = \rho c \dfrac{g(r')g'(r')}{r'} \end{cases} \quad (11)$$

We now consider the linear transformation $r' = a_1 r + a_0$ with $\varepsilon = 0$. Therefore, we want our homogenized cloak to behave like Pendry's cloak. Solving for κ_1 and κ_2 provides us with the parameters to use in the concentric multi-layered cloak:

$$\kappa_1(r') = \frac{r' + \sqrt{R_1(2r'-R_1)}}{r' - R_1}$$
$$\kappa_2(r') = \frac{r' - \sqrt{R_1(2r'-R_1)}}{r' - R_1} \quad (12)$$

Then, we approximate $\kappa_1(r')$ and $\kappa_2(r')$ by dividing radially the cloak into N elements and by taking the mean of $\kappa_1(r')$ and $\kappa_2(r')$ on each element. Also, we will assume $\rho_1 c_1(r') = \rho_2 c_2(r') = \rho' c'$. The Figure 5 shows the evolution of the conductivity and product ρc parameters as one goes from the inner boundary of the cloak ($R_1 = 1.5$ mm) to the outer boundary of the cloak ($R_2 = 3$ mm) for Pendry's 10-layer, 20-layer and 50-layer homogenized cloaks.

In Fig. 6 we compare the *standard deviation ratio* of Pendry's cloak (red), the 10-layer homogenized cloak (green), the 20-layer homogenized cloak (black) and the 50-layer homogenized cloak (magenta) introduced above. We can see that the homogenization process gives good results as the standard deviation ratio of the homogenized cloaks increases with the number of layers used, rising from 10^1 for the 10-layer cloak in the vicinity of the cloak to 10^2 for the 50-layer cloak. As seen previously, we observe for non-zero angular frequency a decrease in the effectiveness which mainly comes from the reference mesh we used. We still see increasing effectiveness for multi-layered cloak as the number of layers goes up.

However, the goal is still far off since we would like to reach a standard deviation ratio of 10^4 to ascertain our homogenized cloaks mimic Pendry's cloak. But we expect this gap between perfect and homogenized cloaks to depend merely on the number of layers used and the asymptotic behaviour of κ_1 around $r' = R_1$. This point is discussed in the next section.

Discussion

To emphasize the effectiveness of the homogenized cloak, we studied a discretized version of the perfect anisotropic Pendry's cloak in (5)
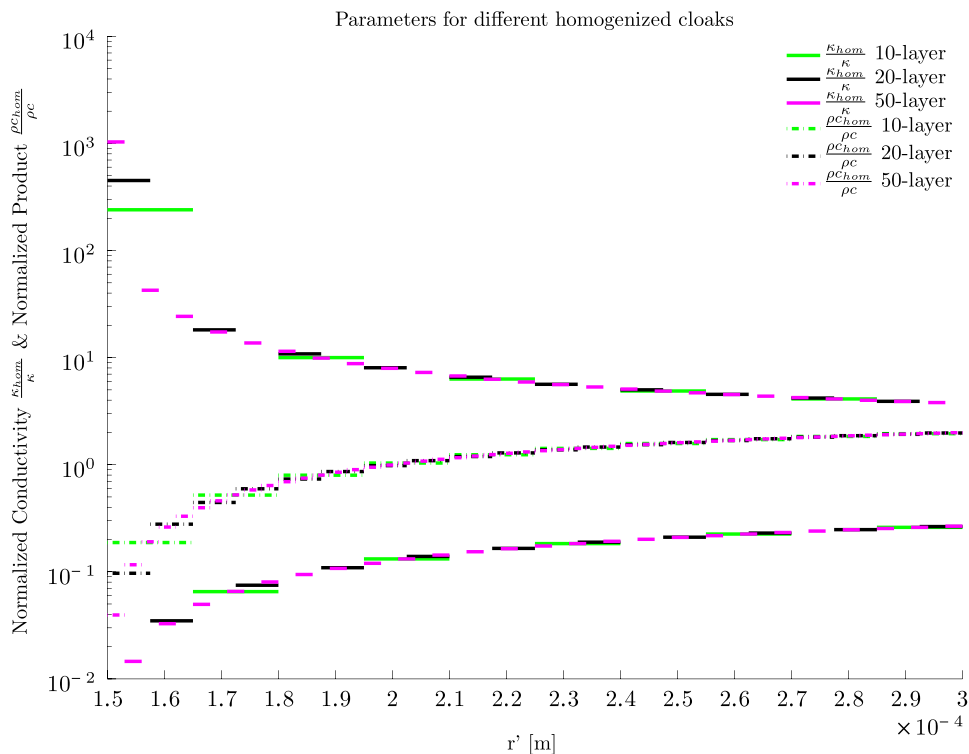
5

Figure 5 | Normalized conductivity $\frac{\kappa_{hom}}{\kappa}$ **and product** $\frac{\rho c_{hom}}{\rho c}$ **parameters used for the Pendry's 10-layer (green), 20-layer (black) and 50-layer (magenta) homogenized cloaks as a function of** r' **inside the cloak (see Table 1 for explicit values used for the 10-layer homogenized cloak).** κ_{hom} denotes either the radial average $< \kappa_1 >$ or $< \kappa_2 >$ depending on the considered radial element. ρc_{hom} denotes the radial average $< \rho' c' >$ on the considered radial element.
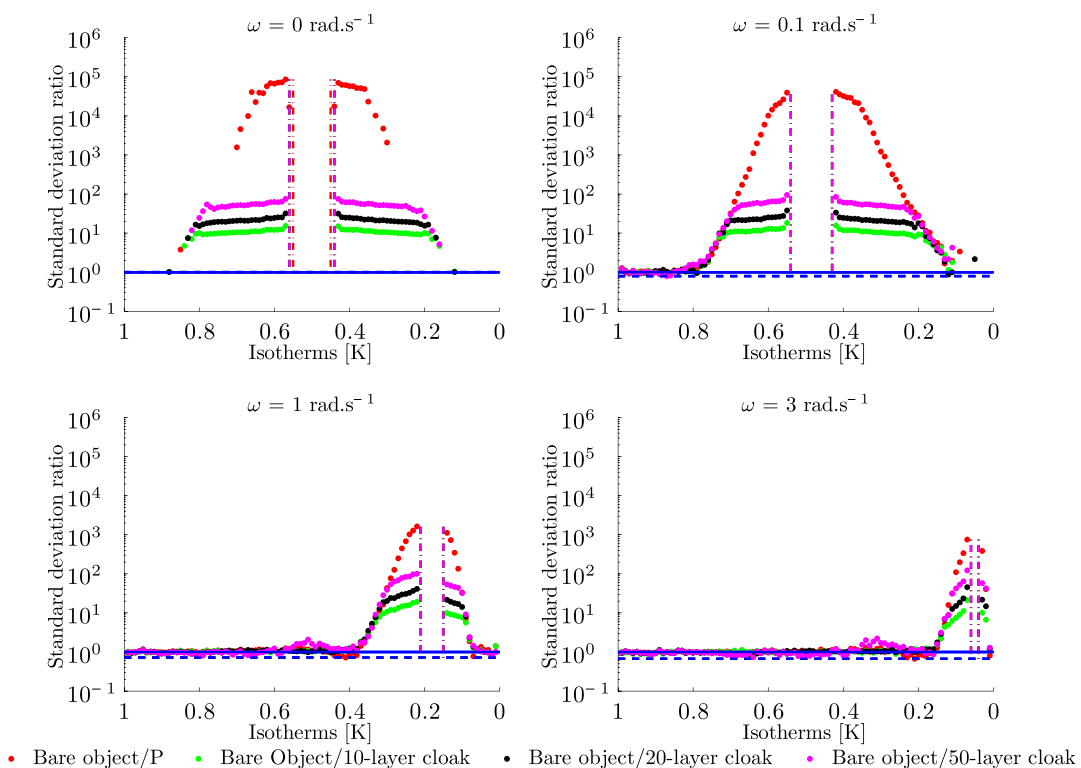

Figure 6 | Standard deviation ratio of Pendry's perfect cloak (red), a 10-layer homogenized cloak (green), a 20-layer homogenized cloak (black) and a 50-layer homogenized cloak (magenta) at angular frequencies $\omega = 0, 0.1, 1$ **and** 3 **rad.s**$^{-1}$**.** The source is on the left so that heat diffuses from left to right. The vertical lines indicate the position of the cloaks. The (z) vertical axis gives the ratio of the deviation on a logarithmic scale, while the (x) horizontal axis is for the temperature of the isotherms. The horizontal dashed blue line indicates the height of minimum of the standard deviation ratio among all the studied cloaks at angular frequency ω.

with $\varepsilon = 0$. We divide the cloak into $N \times M$ elements (N elements in the radial direction and M elements in the azimuthal directions). In each element, we take the average of the conductivity $\underline{\kappa}'$ so that the resulting conductivity in this element can be written

$$\langle \underline{\kappa}' \rangle_{\substack{r_i \to r_{i+1} \\ \theta_i \to \theta_{i+1}}} = \frac{2}{(r_{i+1}^2 - r_i^2)(\theta_{i+1} - \theta_i)} \int_{r_i}^{r_{i+1}} \int_{\theta_i}^{\theta_{i+1}} \underline{\kappa}' \, r \mathrm{d}r \mathrm{d}\theta$$

$$= \begin{pmatrix} \langle \kappa_{11} \rangle & \langle \kappa_{12} \rangle \\ \langle \kappa_{21} \rangle & \langle \kappa_{22} \rangle \end{pmatrix} \quad (13)$$

where r_i and r_{i+1} are the radial boundaries of the element, and θ_i and θ_{i+1} are the azimuthal boundaries of the element. Thus, we obtain a piecewise homogeneous anisotropic cloak. If N and M go to infinity we expect to retrieve the original anisotropic heterogeneous cloak. In Fig. 7, we compare the *standard deviation ratio* of a 50-layer homogenized isotropic cloak and the standard deviation ratio of a 50×5 discretized anisotropic cloak (50 layers in the radial direction and 5 layers in the azimuthal direction), a 50×10 discretized anisotropic cloak and a 50×20 discretized anisotropic cloak. As we can see, we achieve a better effectiveness with the homogenized isotropic cloak than with the discretized anisotropic cloaks, which results from the asymptotic behaviour of $\kappa_{\theta\theta}'$. Thus even compared to the effectiveness of the continuous Pendry's cloak in Fig. 6 (red), it seems that the homogenization process has fairly optimal performances as the discretized anisotropic Pendry's cloak has a much lower effectiveness for the same number of layers. We conclude that achieving effectiveness comparable to that of Pendry's perfect cloak appears to depend merely on the number N of layers used in the homogenized cloak. A finer mesh in the neighbourhood of the cloaks' inner boundary should also improve their effectiveness since this would better fit the rapid change of material parameters.

Finally, we performed numerical simulations to verify the homogenization convergence behaviour as the number of layers N increases. We have the result[17]

$$\|u - u_\varepsilon\|_{L^2} = \sqrt{\int_\Omega |u - u_\varepsilon|^2 \mathrm{d}x} \leq C(\Omega)\varepsilon \quad (14)$$

where u_ε denotes the temperature in the computing domain Ω for a N-layer cloak and u is the limit of u_ε when $\varepsilon \to 0$ (see Sec. Methods). We can also write ε as $\varepsilon = \dfrac{R_2 - R_1}{N}$. Plotting $\log(\|u - u_\varepsilon\|_{L^2})$ as a function of $\log(N)$ should let us verify accordance with equation 14. Also plotting $\log(std(N - layer \; cloak))$ for a given isotherm (the one tangential to the cloak for instance) as a function of $\log(N)$ would give the behaviour of the standard deviation for a given isotherm. The results are plotted on Fig. 8 and are as follows:

Through linear fitting, we find the linear equations

$$\log(\|u - u_\varepsilon\|_{L^2}) \approx -\log(N) + C$$
$$\log(std(N - layer \; cloak)) \approx -\log(N) + C' \quad (15)$$

where C and C' are constants. Thus, we can calculate the number of layers N that would be required to achieve the standard deviation of Pendry'cloak for the same isotherm. Notice that the calculated number of layers N would depend on the mesh that is used (optimized mesh will give an infinite number of layers). We choose the isotherms that are directly tangential to the cloak in the diffusion direction because they are the most difficult to straighten. Direct calculation gives the number of layers required:

$$N = 10^{-\frac{\log(1.4269.10^{-9}) + 4.7561}{1.0178}} = 1,0423.10^4 \quad (16)$$
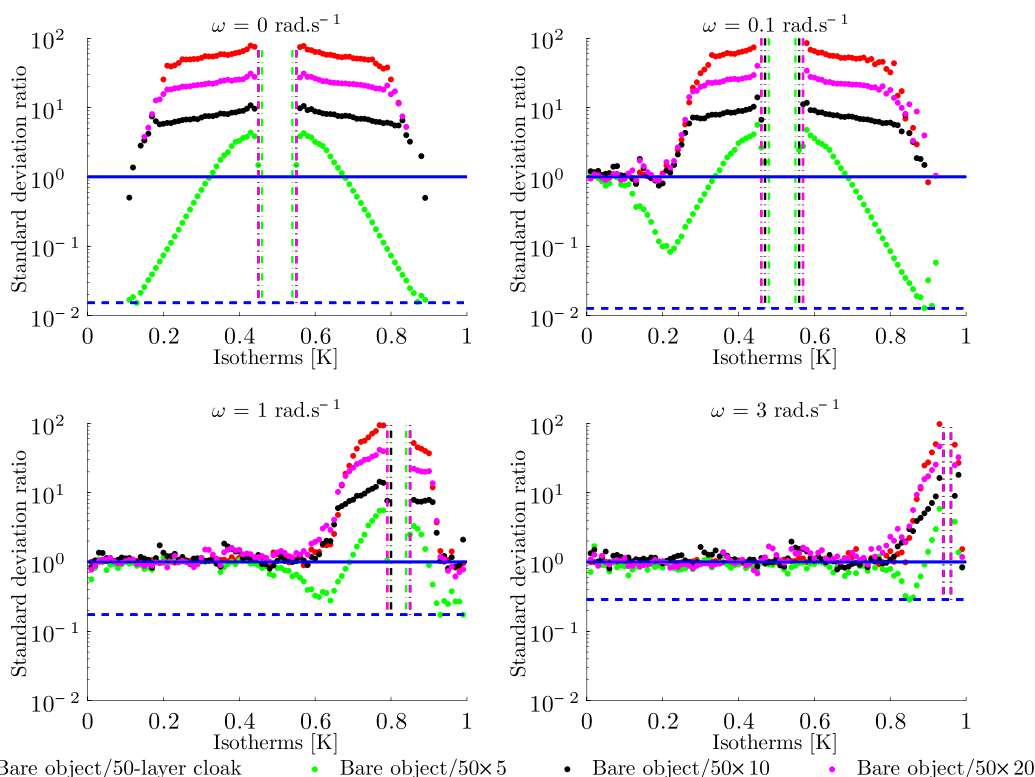

Figure 7 | Standard deviation ratio of a 50-layer homogenized isotropic cloak (red), a 50×5 discretized anisotropic cloak (green), 50×10 discretized anisotropic cloak (black) and a 50×20 discretized anisotropic cloak (magenta) at angular frequencies $\omega = 0, 0.1, 1$ and 3 rad.s^{-1}. The source is on the left so that heat diffuses from left to right. The vertical lines indicate the position of the cloaks. The (z) vertical axis gives the ratio of the deviation on a logarithmic scale, while the (x) horizontal axis is for the temperature of the isotherms. The horizontal dashed blue line indicates the height of minimum of the standard deviation ratio among all the studied cloaks at frequency ω.
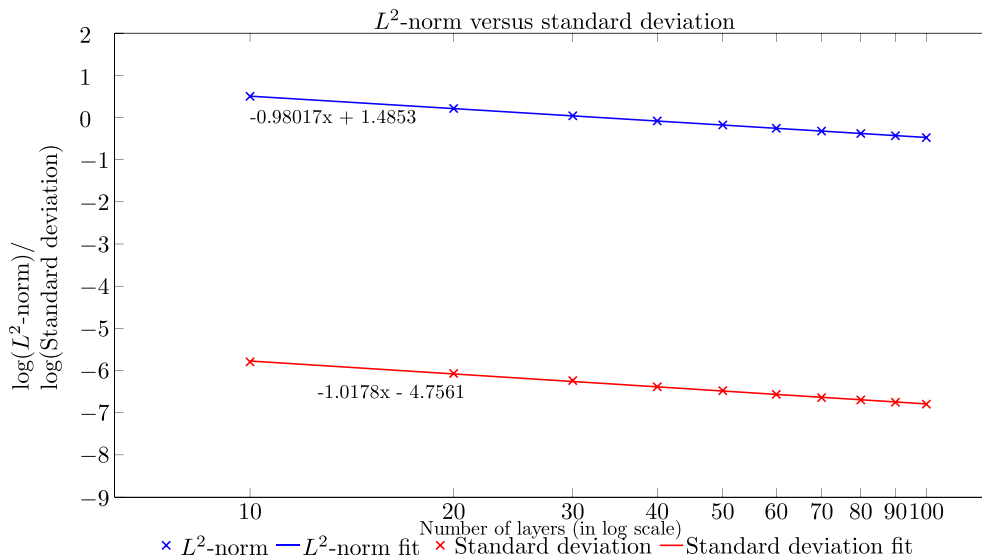
Figure 8 | Logarithm of the L^2-norm (blue) and logarithm of the standard deviation (red), for the isotherm stated before, as a function of log(N) (the values of log(N) have been replaced by the N values for visibility). Simulations are performed at $\omega = 0$ rad.s^{-1}. Linear fit and equations have been added for each curve.

We understand with this high number that building a nearly perfect cloak can be rather difficult as you will need to divide the region $R_2 - R_1$ about ten thousand times. However this study is the first one to shed light on the number of layers in thermal invisibility cloaks and enlightens us on the number of layers that should be used for a certain mesh i.e. for a certain effectiveness tolerance.

We stress that a similar analysis of the effectiveness of electromagnetic invisibility cloaks has not been performed thus far. Hence, we hope that our study will foster theoretical and numerical efforts towards a better understanding of cloak's effectiveness not only in diffusion, but also in wave phenomena.

Methods

Time-harmonic heat equation. We are here interested in a heat source resulting from the absorption of a modulated laser beam, so that the Fourier transform of temperature is introduced as:

$$u(\mathbf{x},\omega) = \int_{-\infty}^{+\infty} T(\mathbf{x},t)e^{-j\omega t}\mathrm{dt} \tag{17}$$

where T is the temperature defined in our computational domain, t the time variable, ω the angular frequency and $\mathbf{x}$ the space variable. We then take the Fourier transform of the heat equation

$$\mathrm{div}(\kappa\nabla T) - \rho c\frac{\partial T}{\partial t} = 0 \tag{18}$$

leading to the time-harmonic heat equation

$$\mathrm{div}(\kappa\nabla u) + j\omega\rho c u = 0 \tag{19}$$

where u is the Fourier transform of the temperature, κ is the conductivity, ρ the density, c the heat capacity and ω the angular frequency of a periodic heat source. Note here that this equation is valid in two and three dimensions.

Standard deviation of isotherms. The Fourier transform of the temperature u can be written like the following

$$u = |u|e^{j\Phi} \tag{20}$$

with Φ depending on the position and the angular frequency ω. Thus, we retrieve the (x, y)-coordinate of the $|u|$ curves using COMSOL Multiphysics® and perform the standard deviation of $|u|$ for every isotherms.

Homogenization process. Following the proposal of Greenleaf and coworkers[18] to apply the two-scale convergence method of G. Allaire[13] and G. Nguetseng[12] in the design of approximate multi-layered cloaks, we derive a set of new effective parameters for a multi-layered heat cloak. We consider an alternation of concentric layers of respective conductivities κ_1 and κ_2 and of respective heat capacities $\rho_1 c_1$ and $\rho_2 c_2$ so that the overall conductivity and heat capacities can be written

$$\kappa_\varepsilon(x) = \kappa_1(x)\mathbb{1}_{[0,1/2]}\left(\frac{r}{\varepsilon}\right) + \kappa_2(x)\mathbb{1}_{[1/2,1]}\left(\frac{r}{\varepsilon}\right)$$
$$\rho_\varepsilon c_\varepsilon(x) = \rho_1 c_1(x)\mathbb{1}_{[0,1/2]}\left(\frac{r}{\varepsilon}\right) + \rho_2 c_2(x)\mathbb{1}_{[1/2,1]}\left(\frac{r}{\varepsilon}\right) \tag{21}$$

where x is the position vector, $r = ||x||$ is the Euclidean norm of x and $\mathbb{1}_I$ is the indicator function of the set I. The function κ_ε is periodic on the set $Y = [0, 1]$ and ε represents its periodicity (clearly, the thinner the layers in the cloak, the smaller the positive parameter ε). In this set of concentric layers, the time-harmonic heat equation is written

$$\mathrm{div}(\kappa_\varepsilon\nabla u_\varepsilon) + j\omega\rho c u_\varepsilon = 0 \tag{22}$$

where u_ε is the Fourier transform of the temperature and ω is the angular frequency of

Table 1 | Conductivity and product ρc parameters used for the 10-layer homogenized cloak after averaging on each radial element				
$r \times 10^{-4}(m)$	1.5–1.65	1.65–1.8	1.8–1.95	1.95–2.1	2.1–2.25
$\frac{\kappa_{hom}}{\kappa}$	240.35	0.07	10.01	0.13	6.30
$\frac{\rho c_{hom}}{\rho c}$	0.19	0.52	0.80	1.04	1.24
$r \times 10^{-4}(m)$	2.25–2.4	2.4–2.55	2.55–2.70	2.70–2.85	2.85–3
$\frac{\kappa_{hom}}{\kappa}$	0.18	4.88	0.23	4.11	0.26
$\frac{\rho c_{hom}}{\rho c}$	1.42	1.58	1.71	1.84	1.95

a periodic heat source. It is possible to show that when $\varepsilon \to 0$, this alternation of materials behaves like an anisotropic inhomogeneous medium of conductivity

$$A^{hom}(x) = \begin{pmatrix} \frac{1}{\int_Y \frac{1}{\kappa_0} dy} & 0 \\ 0 & \int_Y \kappa_0 dy \end{pmatrix} \qquad (23)$$

and heat capacity

$$(\rho c)^{hom}(x) = \int_Y \rho_0 c_0 dy = \frac{1}{2}(\rho_1 c_1 + \rho_2 c_2) \qquad (24)$$

where κ_0 and $\rho_0 c_0$ are the respective two-scale limits of κ_ε and $\rho_\varepsilon c_\varepsilon$ when $\varepsilon \to 0$ and are written

$$\kappa_0(x,y) = \kappa_1(x) \mathbb{1}_{[0,1/2]}(y) + \kappa_2(x) \mathbb{1}_{[1/2,1]}(y)$$
$$\rho_0 c_0(x,y) = \rho_1 c_1(x) \mathbb{1}_{[0,1/2]}(y) + \rho_2 c_2(x) \mathbb{1}_{[1/2,1]}(y) \qquad (25)$$

The homogenized time-harmonic heat equation is then written

$$\text{div}\left(A^{hom}(x)\nabla u(x)\right) + j\omega(\rho(x)c(x))^{hom} u(x) = 0 \qquad (26)$$

where u is the limit of u_ε when $\varepsilon \to 0$. Then, we need to solve the system

$$\begin{cases} A^{hom} = \underline{\kappa}' \\ (\rho c)^{hom} = \rho c \det(\mathbf{J}) \end{cases} \qquad (27)$$

for our set of materials to work as our cloak.

1. Pendry, J. B., Schurig, D. & Smith, D. R. Controlling electromagnetic fields. *Science* **312**, 1780–1782 (2006).
2. Leonhardt, U. Optical conformal mapping. *Science* **312**, 1777–1780 (2006).
3. Guenneau, S., Amra, C. & Veynante, D. Transformation thermodynamics: cloaking and concentrating heat flux. *Opt. Expr.* **20**, 8207–8218 (2012).
4. Schittny, S., Kadic, M., Guenneau, S. & Wegener, M. Experiments on transformation thermodynamics: molding the flow of heat. *Phys. Rev. Lett.* **110**, 195901 (2013).
5. Han, T. *et al*. Experimental demonstration of a bilayer thermal cloak. *Phys. Rev. Lett.* **112**, 054302 (2014).
6. Xu, H., Shi, X., Gao, F., Sun, H. & Zhang, B. Experimental demonstration of an ultra-thin three-dimensional thermal cloak. *Phys. Rev. Lett.* **112**, 054301 (2014).
7. Han, T. *et al*. Full control and manipulation of heat signatures: Cloaking, camouflage and thermal metamaterials. *Adv. Mater.* **26**, 1731–1734 (2014).
8. Guenneau, S. & Puvirajesinghe, T. M. Fick's second law transformed: one path to cloaking in mass diffusion. *J. R. Soc. Inter.* **10**, 20130106 (2013).
9. Lunwu, Z. & Runxia, S. Controlling chloride ions diffusion in concrete. *Sci. Rep.* **3**, 3359 (2013).
10. Schittny, S., Kadic, M., Bückmann, T. & Wegener, M. Invisibility cloaking in a diffusive light scattering medium. *Science* **345**, 427–429 (2014).
11. Han, T., Yuan, T., Li, B. & Qiu, C.-W. Homogeneous thermal cloaks with constant conductivity and tunable heat localization. *Sci. Rep.* **3**, 1593 (2013).
12. Nguetseng, G. A general convergence result for a functional related to the theory of homogenization. *SIAM J. Math. Anal.* **20**, 608–623 (1989).
13. Allaire, G. Homogenization and two-scale convergence. *SIAM J. Math. Anal.* **23**, 1482–1518 (1992).
14. Alú, A. Thermal cloaks get hot. *Physics* **7**, 12 (2014).
15. Milton, G. W., Cai, W., Chettiar, U. K., Kildishev, A. V. & Shalaev, M. V. Nonmagnetic cloak with minimized scattering. *Appl. Phys. Lett.* **91**, 111105 (2007).
16. Kohn, R. V., Shen, H., Vogelius, M. S. & Weinstein, M. I. Cloaking via change of variables in electric impedance tomography. *Inv. Probl.* **24**, 015016 (2008).
17. Pakhnin, M. A. & Suslina, T. A. Operator error estimates for the homogenization of the elliptic Dirichlet problem in a bounded domain. (Russian) *Algebra i Analiz* **24**, no. 6, 139–177 (2012), translation in *St. Petersburg Math. J.* **24**, no. 6, 949–976 (2013).
18. Greenleaf, A., Kurylev, Y., Lassas, M. & Uhlmann, G. Isotropic transformation optics: approximate acoustic and quantum cloaking. *New J. Phys.* **10**, 115024 (2008).

Acknowledgments

Author contributions

D.P., S.G. and C.A. wrote the main manuscript text. M.B. provided help for the homogenization process method. M.Z. prepared figure 2 (left and right). All authors reviewed the manuscript.

Additional information

Competing financial interests: The authors declare no competing financial interests.